Protoplasma (2006) 227: 185–196
DOI 10.1007/s00709-005-0139-x

PROTOPLASMA
Printed in Austria

Intranuclear accumulation of plant tubulin in response to low temperature

K. Schwarzerová[1,*], **J. Petrášek**[1,2], **K. C. S. Panigrahi**[3], **S. Zelenková**[1], **Z. Opatrný**[1], and **P. Nick**[4]

[1] Department of Plant Physiology, Faculty of Science, Charles University, Prague
[2] Institute of Experimental Botany, Academy of Sciences of the Czech Republic, Prague
[3] Institut für Biologie II, University of Freiburg, Freiburg
[4] Botanisches Institut 1, University of Karlsruhe, Karlsruhe

Received February 14, 2005; accepted June 4, 2005; published online May 3, 2006

Summary. Concurrently with cold-induced disintegration of microtubular structures in the cytoplasm, gradual tubulin accumulation was observed in a progressively growing proportion of interphase nuclei in tobacco BY-2 cells. This intranuclear tubulin disappeared upon rewarming. Simultaneously, new microtubules rapidly emerged from the nuclear periphery and reconstituted new cortical arrays, as was shown by immunofluorescence. A rapid exclusion of tubulin from the nucleus during rewarming was also observed in vivo in cells expressing GFP-tubulin. Nuclei were purified from cells that expressed GFP fused to an endoplasmic-reticulum retention signal (BY-2-mGFP5-ER), and green-fluorescent protein was used as a diagnostic marker to confirm that the nuclear fraction was not contaminated by nuclear-envelope proteins. These purified, GFP-free nuclei contained tubulin when isolated from cold-treated cells, whereas control nuclei were void of tubulin. Furthermore, highly conserved putative nuclear-export sequences were identified in tubulin sequences. These results led us to interpret the accumulation of tubulin in interphasic nuclei, as well as its rapid nuclear export, in the context of ancient intranuclear tubulin function during the cell cycle progression.

Keywords: Tobacco Bright Yellow 2; Microtubule; Nucleus; Plant cell; Tubulin.

Abbreviations: NLS nuclear-localization sequence; NES nuclear-export sequence.

Introduction

The microtubular cytoskeleton plays a dual role during the progression of the cell cycle. In interphase, microtubules are exclusively found in the cytoplasm, where they participate in intracellular transport, distribution of organelles, and maintenance of cell shape. Depending on the phase of the cell cycle, microtubules are organized in different structures – cortical microtubular arrays at G_1, cortical and endoplasmic microtubules at S and G_2 phase, preprophase band of microtubules at late G_2 phase – being, however, always confined to the cytoplasm and separated from the karyoplasm. When the nuclear envelope disintegrates at the onset of mitosis, the organized scaffold of microtubules disappears. The division spindle is established and the major role of microtubules is to ensure an equal distribution of genetic material between the two daughter cells. After the completion of nuclear division and reformation of the nuclear envelope, a new cytoplasmic interphase array of microtubules is reestablished (Hasezawa and Kumagai 2002).

The microtubular structures listed above differ not only with respect to their timing but also with respect to their nucleation. In contrast to animal and plant cells, some protists, fungi, and algae perform a so-called closed mitosis, where nuclear division takes place within an intact nuclear envelope (for a review, see Heath 1980). In cells with closed mitosis, the entry of tubulin and microtubule-nucleating components into the nucleus at the onset of mitosis, as well as their exclusion at the end, must be under strict cell cycle control. For example, in *Saccharomyces cerevisiae*, microtubules of the mitotic spindle are organized inside the nucleus by a specialized structure, the spindle pole body (SPB) (Pereira et al. 1998). It has been shown that the SPB assembles in the cytoplasm and is transported in a cell cycle-dependent manner into the nucleus via the nuclear-localization sequence (NLS) of

* Correspondence and reprints: Department of Plant Physiology, Faculty of Science, Charles University, Viničná 5, 128 44 Prague 2, Czech Republic. E-mail: schwarze@natur.cuni.cz

Spc98p protein (Pereira et al. 1998). Interestingly, α- and β-tubulin, the basic components of the mitotic spindle, are not found in the nucleus of cells with closed mitosis during interphase. Therefore, in organisms with closed mitosis, tubulin has to be transported into and out of the nucleus. Indeed, it has been shown in *Aspergillus nidulans* that tubulin enters the nucleus immediately before the onset of closed mitosis and is quickly excluded at the end (Ovechkina et al. 2003). Although the molecular mechanisms of nuclear tubulin transport remain to be elucidated, these results suggest that the movement of tubulin through the nuclear envelope during the cell cycle is an active and highly regulated process.

The mitotic spindle microtubules of animals, higher plants (Embryobionta), and charophycean green algae (Charophyceae) interact with chromosomes after the nuclear envelope has disintegrated at the onset of mitosis (Heath 1980). Consequently, directed movement of tubulin through the nuclear envelope is not required for formation of the mitotic spindle. After nuclear envelope disintegration, the microtubular spindle can exploit the pool of cytoplasmic tubulin that is no longer withdrawn by compartmentalization. The spindle microtubules are nucleated from centrosomes in animal and algal cells (Wiese and Zheng 1999), but from rather diffuse microtubule-organizing centers (MTOCs) in the acentriolar cells of higher plants (Baskin and Cande 1990, Shimamura et al. 2004). In addition, the kinetochores of both animal and plant cells are endowed with a microtubule-nucleating activity (Cande 1990). γ-Tubulin, a minus-end nucleator of microtubule assembly, is an indispensable component of both centrosomes and plant MTOCs (Pereira and Schiebel 1997, Stoppin-Mellet et al. 2000). In plant cells, the association of γ-tubulin with the prospective kinetochore sites already occurs during the G_2 phase and thus precedes the disintegration of the nuclear envelope (Binarová et al. 2000). This indicates that, like the SPB of *S. cerevisiae*, the microtubule-nucleating component γ-tubulin must be actively transported through the intact nuclear envelope before mitosis. Again, neither the molecular mechanism of γ-tubulin transport into the nucleus is known nor whether other components of MTOCs persist in the nucleus during the whole cell cycle or have to be imported as well.

In our previous work, we followed the response of the microtubular and actin cytoskeleton to low temperature in tobacco cells (Pokorná et al. 2004). We observed a progressive disintegration of microtubules during prolonged exposure of tobacco BY-2 cells to 0 °C and a reassembly of microtubules during subsequent recovery at 25 °C. In the present work, we show by means of several methods that cold-induced disintegration of microtubules is accompanied by the entry of tubulin into the interphase nuclei and its gradual accumulation there. Upon rewarming, tubulin was quickly excluded from the nuclei and immediately polymerized into cytoplasmic microtubules such that free tubulin became undetectable in most nuclei within a few minutes of incubation at 25 °C. The accumulation of tubulin in nuclei and its exclusion from them were shown by immunofluorescence staining and also in vivo in cells that expressed GFP–α-tubulin. Furthermore, increasing levels of α-tubulin could be detected in isolated and highly purified nuclei during cold treatment. We interpret these findings first of all as evidence for a reversible permeabilization of the nuclear envelope for tubulin, possibly via altered function of nuclear pore complexes (NPCs). Further, these data indicate intranuclear tubulin-binding sites that are either unmasked or activated under certain environmental conditions. The subsequent quick exclusion of tubulin from interphase plant nuclei during rewarming could be explained by the recovery of tubulin transport between karyo- and cytoplasm and seems to be an active process. This is supported by the identification of five putative signatures for nuclear export in sequences of plant α- and β-tubulin. This transport might be functionally relevant for the dynamic changes in the nuclear envelope at the beginning and end of mitosis.

Material and methods

Plant material and chemicals

The tobacco cell line BY-2 (*Nicotiana tabacum* L. cv. Bright Yellow 2 [Nagata et al. 1992]) was cultured in medium containing 4.3 g of Murashige–Skoog salts (Sigma, St. Louis, Mo., U.S.A.), 1 mg of thiamine, 200 mg of KH_2PO_4, 100 mg of myo-inositol, 30 g of sucrose, and 0.2 mg (0.9 μM) of 2,4-dichlorophenoxyacetic acid (2,4-D) per liter, pH 5.8. The transgenic BY-2 cell lines GT16, expressing GFP–α-tubulin (Kumagai et al. 2001), and BY-2-mGFP-ER, expressing mGFP5-ER (Petrášek et al. 2003), were maintained on the same medium supplemented with 100 μg of kanamycin and 100 μg of cefotaxim per ml. Every 7 days, 1.5 ml of cells were transferred to 30 ml of fresh medium and cultured in darkness at 25 °C on an orbital shaker (IKA KS501; IKA Labortechnik, Staufen, Federal Republic of Germany; 120 rpm; orbital diameter, 30 mm). All chemicals were obtained from Sigma unless stated otherwise.

Cold treatment and recovery experiments

Cells in the exponential phase of growth (3 days after inoculation) were used for all experiments. Cell suspensions in Erlenmeyer flasks were placed in a bath of ice water to maintain the temperature at 0 °C and shaken on an orbital shaker at 100 rpm (IKA KS501) in darkness. For recovery experiments, flasks were taken from the ice water and the cells were immediately collected by filtering through a nylon mesh (mesh diameter, 20 μm). They were then resuspended in conditioned medium at optimal temperature (25 °C) that had been obtained by sterile filtration

of 3-day-old BY-2 cells. Thereafter, the cells were cultivated at 25 °C. Samples of cells for cytological observation or extraction of proteins were taken at specified time points during the cold treatment and subsequent recovery at normal temperature.

Observation of tubulin exclusion from nuclei in vivo

The tobacco cell line expressing GFP-tubulin was cultivated at 0 °C as described above. For observation under the confocal laser scanning microscope, a drop of cell suspension was collected from the flask and placed on a prewarmed (25 °C) microscopic slide. The drop of cell suspension was covered immediately with a coverslip and observed under a confocal laser scanning microscope (Leica TCS NT, Heidelberg, Federal Republic of Germany). The optimal confocal plane through the nuclear region of a selected cell or cell file was defined and a time-lapse sequence was recorded at this confocal plane. The time-lapse scanning was recorded over 20 min at 1 min intervals.

To measure the exclusion of tubulin from the nucleus and its accumulation in the cytoplasm around the nucleus during the recovery period, the first and last confocal sections from time-lapse series were analyzed. The intensity of the tubulin signal was measured by the Scion Image program (Scion Corporation, Frederick, Md., U.S.A.) using a linear probe (profile plot line width, 6) that was placed so as to cover the nuclear region, the cytoplasm around the nucleus, and the vacuolar region with one probe. Intensity profiles were plotted onto graphs and the respective parts of curves were labeled as nucleus, cytoplasm, and vacuole.

Visualization of microtubules

Microtubules were visualized as described by Wick et al. (1981) with the modifications described by Mizuno (1992). Briefly, 3 ml of cell suspension (at day 3 after inoculation) were prefixed for 10 min at 25 °C in 3.7% (w/v) paraformaldehyde (PFA) in microtubule-stabilizing buffer (MSB), consisting of 50 mM piperazine-1,4-bis(2-ethanesulfonic acid), 2 mM ethylene-bis(oxyethylenenitrilo)tetraacetic acid, and 2 mM $MgSO_4 \cdot 7H_2O$, pH 6.9, followed by fixation in 3.7% (w/v) PFA with 1% Triton X-100 in MSB for 50 min. For cold-treated cells, fixation for the first 10 min was performed in fixation solution chilled to 0 °C. After digestion with an enzyme solution (1% [w/v] macerozyme and 0.1% [w/v] pectolyase) for 7 min at 25 °C, the cells were attached to poly-L-lysine-coated coverslips and treated with 1% (v/v) Triton X-100 in MSB for 20 min. Subsequently, the cells were treated with 0.5% (w/v) bovine serum albumin (Fluka, Buchs, Switzerland) in phosphate-buffered saline (PBS) (8 g of NaCl, 0.2 g of KCl, 0.158 g of KH_2PO_4, 2.31 g of $Na_2HPO_4 \cdot 12\ H_2O$ per liter) for 30 min and incubated with a monoclonal mouse antibody against α-tubulin (N356; Amersham Biosciences Europe GmbH, Freiburg, Federal Republic of Germany) for 45 min at 25 °C (1 : 500 dilution in PBS). After washing with PBS, a secondary FITC (fluorescein isothiocyanate)- or TRITC (tetramethylrhodamine isothiocyanate)-conjugated anti-mouse antibody, diluted 1 : 80 in PBS, was applied for 1 h at 25 °C. The specimens were washed in PBS, embedded in 50% glycerol supplemented with 0.1 μg of bisbenzimide (2′-(4-ethoxyphenyl)-5-(4-methyl-1-piperazinyl), Hoechst 33258) to stain nuclei, and viewed immediately.

Microscopy and image processing

Immunolabeled samples were viewed under an epifluorescence microscope (Olympus Provis AX 70; Olympus Optical Co., Ltd., Japan) equipped with appropriate filter sets for the detection of TRITC (excitation at 510–550 nm, barrier filter at 590 nm), FITC (excitation at 450–480 nm, barrier filter at 515 nm), and Hoechst 33258 fluorescence (excitation at 330–385 nm, barrier filter at 420 nm). Objective lenses used were Plan Apo (magnification, ×40; numerical aperture, 0.85) or LUMPlan Fl (magnification, ×40; numerical aperture, 0.80). The fluorescence signal was grabbed with a monochromatic integrating charge-coupled-device camera (Cohu 4910; Cohu, Inc., Poway, Calif., U.S.A.) and Nomarski differential interference contrast (DIC) images were taken with a 3-charge-coupled-devices color-video camera (Sony DXC-950P; Sony Corp., Tokyo, Japan). Images were digitally stored using the Lucia image analysis software (Laboratory Imaging, Prague, Czech Republic). Optical sections were obtained with a confocal laser scanning microscope (Leica TCS NT) equipped with an ArKr laser using filter sets for GFP (excitation at 488 nm, emission at 515–545 nm), FITC (excitation at 488 nm, emission at 515–545 nm), and TRITC (excitation at 568 nm, emission at 590 nm). An objective lens Plan Apo (magnification, ×63; numerical aperture, 1.2) was used for all observations.

For the determination of the percentage of cells containing tubulin in nuclei during cold treatment, at least 200 cells were assessed in total for each sample. During image grabbing, the setup of the frame grabber and the intensity of the fluorescence lamp were optimized for control cells with no signal in the nucleus and all other samples were grabbed with this setup. Therefore, all obtained values are corrected to this "base line". Cells in which the tubulin signal was stronger in nuclei, but not in nucleoli, as compared to the cytoplasm (refer to Figs. 1C, D and 2A, C″), were considered as containing tubulin in nuclei. All other cells were considered as not containing tubulin in nuclei.

Isolation of nuclei

All procedures were performed at 4 °C unless stated otherwise. 100 ml of BY-2-mGFP5-ER cells in exponential phase (3 days after inoculation) were collected by filtering through a nylon mesh (mesh diameter, 20 μm) and subsequently resuspended in 10 volumes of chilled buffer A (10 mM Tris-HCl, pH 6.8; complemented with 5 mM $MgCl_2$, 10 mM β-mercaptoethanol, 0.15 M sucrose, 50% [v/v] glycerol, 1 mM phenylmethylsulfonyl fluoride, 50 μM N-*p*-tosyl-L-phenylalanine chloromethyl ketone, and 0.6% [v/v] Triton X-100). Cells were homogenized in a Waring blender for 30 s and filtered through Miracloth (Calbiochem, Merck Biosciences Ltd., Nottingham, U.K.). Cell material retained by the filter was collected and resuspended in 10 volumes of buffer A, homogenized once again for 30 s, and filtered through Miracloth. Filtrates were mixed and filtered through a nylon mesh (mesh diameter, 20 μm). The filtrate was centrifuged at 500 **g** for 5 min at 2 °C, and the resulting supernatant was centrifuged again at 2000 **g** for 10 min at 2 °C. An aliquot of 100 μl was collected from the supernatant and stored at −20 °C as fraction I. The sediment containing nuclei was resuspended carefully in 1 ml of cold buffer A, and again an aliquot of 100 μl was collected as fraction II. Nuclei were further purified by centrifugation through a 25% to 50% Percoll gradient prepared in buffer A at 7000 **g** for 30 min at 2 °C. The interface which contained the nuclei was collected, resuspended in 15 ml of buffer A, and centrifuged at 4000 **g** for 10 min at 2 °C. Sedimented nuclei were washed with buffer A and centrifuged at 2000 **g** for 10 min at 2 °C. Again, an aliquot of 100 μl was collected from the supernatant as fraction III. The sedimented nuclei (fraction IV) were assayed under the microscope and proteins were extracted and separated electrophoretically.

Protein electrophoresis and immunoblotting

Proteins from fractions I–IV were precipitated with 10% trichloroacetic acid and diluted in denaturing sample buffer (50 mM Tris-HCl, pH 6.9, 2% [w/v] SDS [sodium dodecyl sulfate], 36% [w/v] urea, 30% [w/v] glycerol, 5% [v/v] β-mercaptoethanol, 0.5% [w/v] bromophenol blue). The total concentration of proteins was determined after staining with amido black (Popov et al. 1975). Protein samples were vortexed, boiled for 5 min and separated by SDS polyacrylamide gel electrophoresis (PAGE) on 10% (v/v) acrylamide gels. The separated proteins were transferred onto polyvinylidene difluoride membranes by electro-blotting (SemiDry, Bio-Rad) and probed with antibodies. For the Western

blot analyses, we used the mouse monoclonal anti-α-tubulin antibody N356 (Amersham Biosciences) at 1 : 4000 dilution, the mouse monoclonal anti-tyrosinated α-tubulin antibody TUB-1A2 (Sigma) at 1 : 800 dilution, and the mouse monoclonal anti-GFP antibody (mixture of clone 7.1 and 13.1; Boehringer Mannheim GmbH, Mannheim, Federal Republic of Germany) at 1 : 1000 dilution. After incubation with an anti-mouse horseradish peroxidase-conjugated secondary antibody (ICN Biochemicals), the proteins were visualized by means of a chemiluminiscence ECL detection kit (Amersham Biosciences) on X-ray films (Foma, Hradec Králové, Czech Republic). The polyvinylidene difluoride membrane with the blotted proteins was stained with amido black.

Identification of potential nuclear-export sequences

All reported amino acid sequences of *Arabidopsis thaliana* α- and β-tubulin and three known amino acid sequences of *Nicotiana tabacum* α-tubulin (nucleotide database at National Center for Biotechnology Information website http://www.ncbi.nlm.nih.gov/) were scanned by eye to identify nuclear-export sequences that correspond to a consensus as follows: Z-X(1–4)-J-X(2–3)-Z-X-Z, where Z stands for Leu (L), Ile (I), or Val (V); J stands for Z, Met (M), or Phe (F); X stands for any (Mirski et al. 2003).

Results

Tubulin accumulates in the nucleus during chilling

At the control temperature of 25 °C, the microtubular cytoskeleton of interphase tobacco BY-2 cells was arranged in the classical pattern of transversely oriented microtubules. Tubulin was present exclusively as polymerized microtubules in the cortical cytoplasm, not in the nuclei, as observed by confocal laser scanning microscopy (Fig. 1A, A′; nucleus, Fig. 1A″). Cortical microtubules were clearly affected after 1 h of chilling at 0 °C (Fig. 1B) and a diffuse tubulin signal accumulated progressively around the nuclei (Fig. 1B′, B″), although it was largely excluded from the karyoplasm. However, weak staining of nuclei in Fig. 1B′ might reflect early stages of intranuclear tubulin accumulation. The first clear incidence of intranuclear tubulin was detected after around 4 h of chilling (Fig. 1G). During prolonged chilling (up to 12 h), the cortical microtubules disappeared progressively, whereas the frequency of cells with intranuclear tubulin increased steadily, reaching approximately 50% after 12 h of chilling. Tubulin appeared to be present throughout the karyoplasm in a diffuse or very fine punctate pattern but was clearly absent from the nucleoli (Fig. 1C, C′ for epifluorescence microscopy, Fig. 1D for confocal laser scanning microscopy). Cells that were presumably in mitosis at the time of the shift to 0 °C exhibited depolymerized mitotic spindles, leading to a diffuse tubulin signal surrounding the spiralized chromosomes (Fig. 1E, E′). The number of cells with intranuclear tubulin increased during the 12 h of chilling (Fig. 1G).

In order to test whether the elimination of cytoplasmic microtubules would generally result in accumulation of tubulin in nuclei, the cells were treated with 5 μM oryzalin. Microtubules were effectively removed after 11 h of this treatment (Fig. 1F). A diffuse tubulin signal accumulated near the nuclei but clearly remained excluded from the karyoplasm as shown by double staining with Hoechst 33258 (Fig. 1F′).

New microtubules are rapidly nucleated from nuclear tubulin upon rewarming

After 7 h of cold treatment, cells retained only very few microtubules in the cortical region, but up to 25% of cells exhibited a massive tubulin signal in the nuclei (Fig. 2A, A′). However, upon rewarming, new microtubules were initiated within a few seconds on the surface of the nuclei, and a reticular array developed around the nucleus within 10 min after the temperature had been raised (Fig. 2B, B′). At the same time, the tubulin signal decreased in the nucleus. However, transient stages with newly polymerized microtubules in the cortical cytoplasm (Fig. 2C) and around the nucleus (Fig. 2C′), and a persistent intranuclear tubulin signal (Fig. 2C″, C‴) were observed as well. Note that even in such cells, tubulin remained excluded from the nucleoli. The re-formation of new microtubules was most pronounced at the nuclear surface of early G_1 nuclei (Fig. 2D, D′). Similarly, upon rewarming, new mitotic spindle microtubules were polymerized around the spiralized chromosomes (Fig. 2E, E′). Within 30 min of incubation at 25 °C, the microtubular cytoskeleton had completely recovered in all surviving cells (Fig. 2F, F′) and was almost indistinguishable from that of control cells that had not been challenged by chilling (compare Fig. 2A, A′). Conversely, the intranuclear tubulin had almost completely disappeared (Fig. 2F′, F″).

Tubulin exclusion from nuclei can be followed in vivo within a few minutes of rewarming

To observe tubulin accumulation during cold treatment and its exclusion from nuclei to the cytoplasm during rewarming in vivo, we used the transgenic BY-2 cell line GT16 that expresses GFP-tubulin (Kumagai et al. 2001). Tubulin accumulated in the nuclei of a gradually increasing number of transgenic cells during cultivation at 0 °C, as observed under the confocal microscope (Fig. 3A). Fluorescence intensity profiles measured within the linear probe showed that the GFP signal in cold-treated cells was more intense in the nuclear region than in the

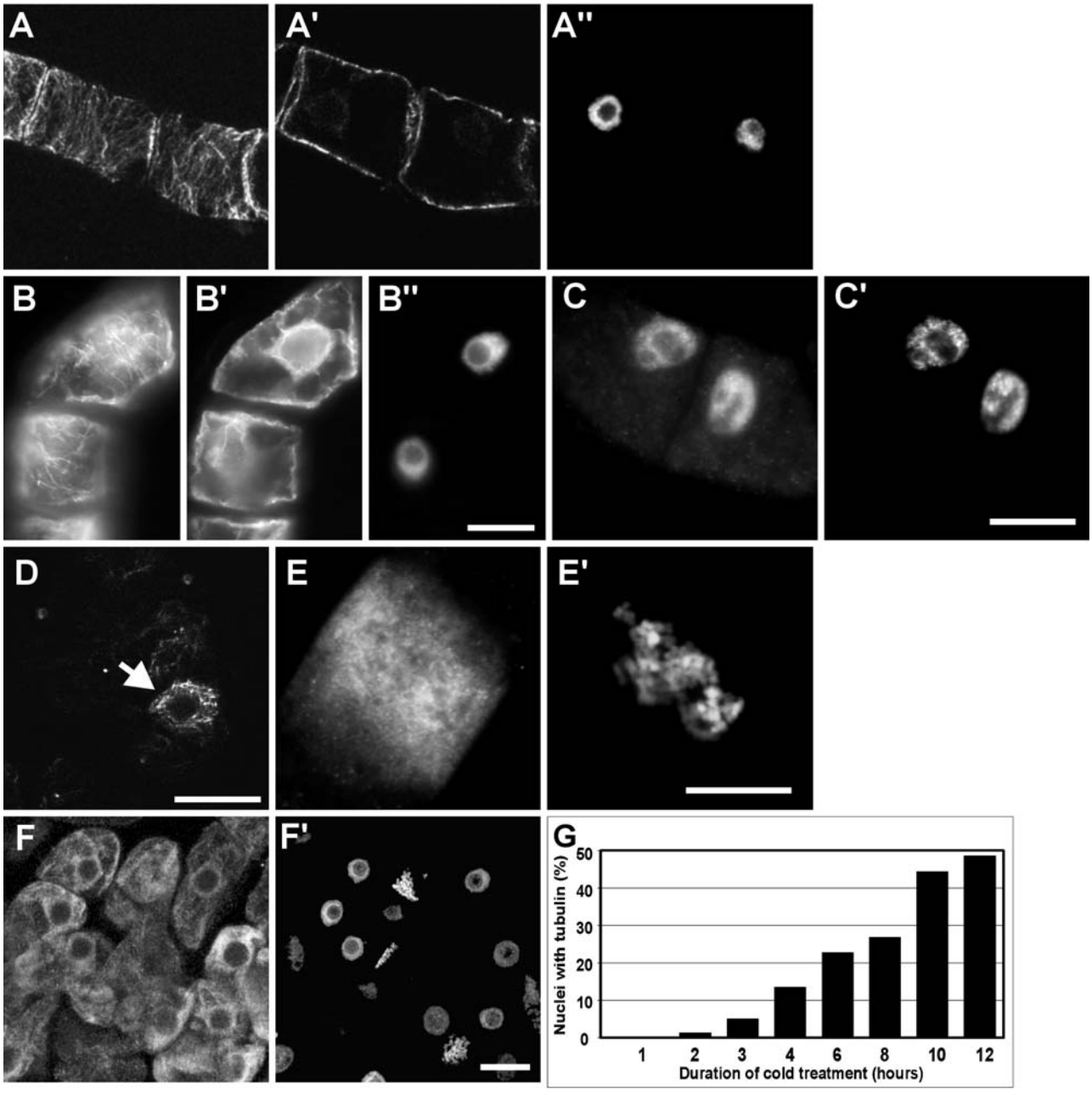

Fig. 1 A–G. α-Tubulin accumulates in nuclei during the response to chilling (0 °C). Microtubules (**A**, **A′**, **B**, **B′**, **C**, **D**, **E**, and **F**) were visualized by immunofluorescence with a monoclonal anti-α-tubulin antibody and a TRITC-conjugated secondary antibody, and DNA was stained with Hoechst 33258 (**A″**, **B″**, **C′**, **E′**, and **F′**) at 0 (**A–A″**), 1 (**B–B″**), 7 (**C**, **C′** and **E**, **E′**), and 12 h (**D**) of chilling, and after 11 h of treatment with 5 μM oryzalin (**F** and **F′**). Cells were observed by conventional epifluorescence microscopy (**B–C′**, **E**, and **E′**) and confocal laser scanning microscopy (**A–A″**, **D**, **F**, and **F′**). Panels A–A″ and B–B″ show two focal planes, one cortical (A and B) and one central (A′, A″, B′, and B″). Panel D shows a central confocal optical section, the arrow indicates position of the nucleus. Panels E and E′ show a residual mitotic spindle around spiralized metaphase chromosomes. Panels F and F′ show four merged optical sections (Z step size, 1 μm) through central regions of cells. Bars: 20 μm. **G** Frequency of cells with intranuclear tubulin during cold treatment. Average values, n = 200 cells per sample

perinuclear cytoplasm (Fig. 3a). Upon rewarming, tubulin was quickly excluded from the nucleus into the cytoplasm (Fig. 3B) and after 20 min at 25 °C, the GFP signal was stronger in the cytoplasm than in the nucleus (Fig. 3b). In control cells, the GFP-tubulin signal was detectable in the perinuclear cytoplasm as a diffuse signal. However, a much weaker GFP signal was always detectable in nuclei (Fig. 3C, c), which was possibly caused by unfused GFP that is present at a low level in transgenic cells (detected on Western blots using anti-GFP antibody, data not

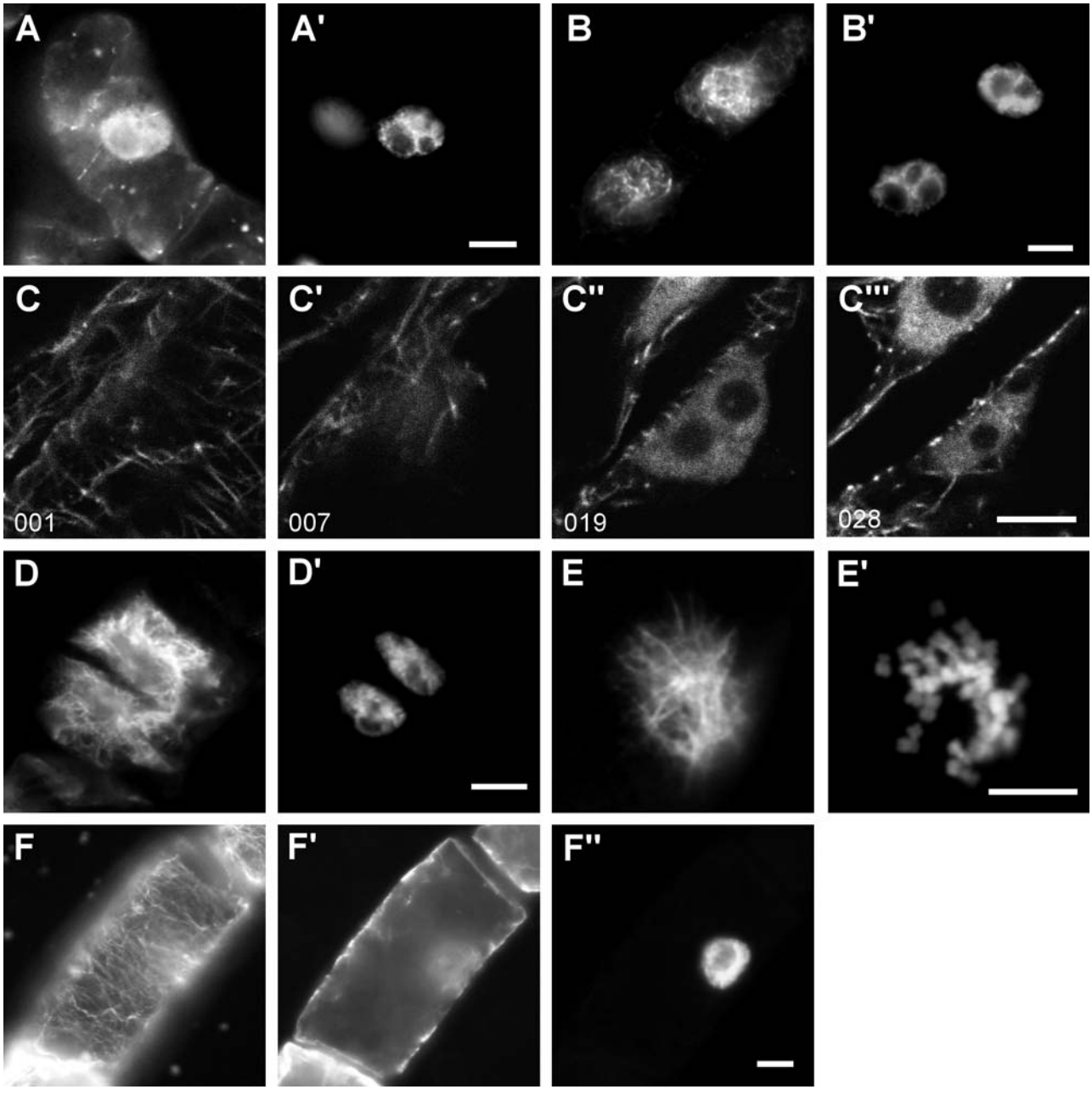

Fig. 2 A–F. Intranuclear α-tubulin disappears simultaneously with the reconstitution of cortical microtubules during rewarming. Tobacco BY-2 cells were subjected to chilling for 7 h at 0 °C and subsequently returned to 25 °C. Microtubule images are shown in panels A, B, C–C‴, D, E, F, and F′; DNA images in panels A′, B′, D′, E′, and F″. For details of staining refer to Fig. 1. **A–C** and **F** Interphase nuclei after 7 h at 0 °C (**A** and **A′**) and after 2 (**C–C‴**), 10 (**B** and **B′**) and 30 min (**F–F″**) of recovery. **D** and **E** Cells in early G_1 (**D** and **D′**) and a reconstituted mitotic spindle (**E** and **E′**) are shown after 5 min of recovery. Cells were observed by conventional epifluorescence microscopy (A–B′, D–F″). **C–C‴** Sequential images were recorded by confocal laser scanning microscopy from a Z-stack taken after 10 h chilling at 0 °C and subsequent rewarming at 25 °C for 2 min. Partial recovery of microtubules can be seen in the cortical region as well as on the nuclear surface (optical sections 1 and 7). However, intranuclear tubulin is still detectable at this stage of recovery (optical sections 19 and 28). Bars: 10 μm

shown) and that can freely pass through nuclear pores (Haseloff et al. 1997). Even after 20 min of observation under the confocal microscope, the ratio between perinuclear, cytoplasmic, and intranuclear GFP signals did not change in the control, with the GFP signal remaining strongest in the cytoplasm (Fig. 3D, d). This suggests that the reduction in the GFP signal observed during recovery at 25 °C after chilling was caused by an active exclusion of tubulin from the nucleus and not due to laser-induced bleaching of GFP during observation.

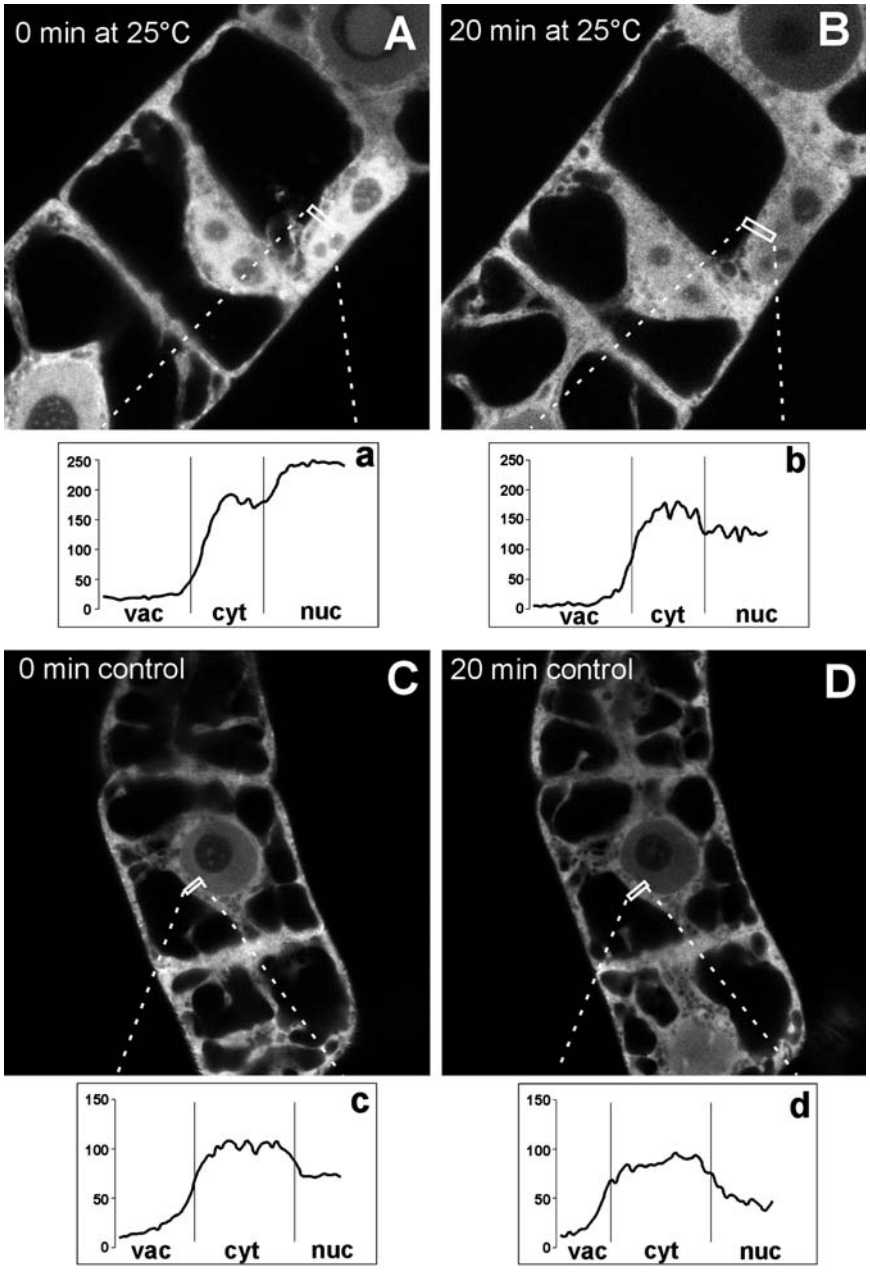

Fig. 3 A, B. Exclusion of tubulin from nuclei during recovery in vivo. **A** and **B** Tobacco cells expressing GFP-tubulin were cultivated at 0 °C for 8 h and then subsequently at 25 °C for 20 min. **A** Confocal optical section in the nuclear region of cells cultivated for 8 h at 0 °C. **B** The same confocal optical section of the same cell after 20 min of recovery at 25 °C. **a** The intensity of the GFP signal was maximal in nuclei of cold-treated cells suggesting that tubulin accumulated in the nuclei during cold treatment. **b** Tubulin was excluded from the nuclei during recovery at 25 °C and accumulated in the surrounding cytoplasm. **C** and **D** A control cell expressing GFP-tubulin kept at 25 °C throughout the experiment. **C** and **D** Confocal optical section in the nuclear region at time zero (**C**) and after 20 min (**D**). **c** The intensity of the GFP signal was maximal in the cytoplasm surrounding nuclei; **d** this distribution of GFP fluorescence did not change during the 20 min of observation. *vac* Vacuole, *cyt* cytoplasm, *nuc* nucleus

Tubulin cofractionates with nuclei from cold-treated cells

The immunofluorescence and in vivo analyses showed that tubulin accumulated in the nuclei of cold-treated cells. To challenge this finding, protein extracts from isolated nuclei of the BY-2 cell line BY-2-mGFP5-ER (Petrášek et al. 2003) were analyzed by Western blotting using monoclonal antibodies recognizing α-tubulin in general, and tyrosinated α-tubulin in particular (for details refer to Wiesler et al. [2002]). Whereas tubulin could not be detected in control nuclei, it was clearly present in nuclei from cold-treated cells (Fig. 4A, B). The nuclear signal of α-tubulin and its tyrosinated form increased progressively with the duration of chilling (Fig. 4A, B, compare extracts taken after 8 and 12 h), in agreement with the increased frequency of tubulin-containing nuclei found in the immunofluorescence study (Fig. 1G). Figure 4C shows an amido black stain of proteins separated by SDS-PAGE and blotted in parallel under the same conditions.

Furthermore, we tested whether the tubulin signal

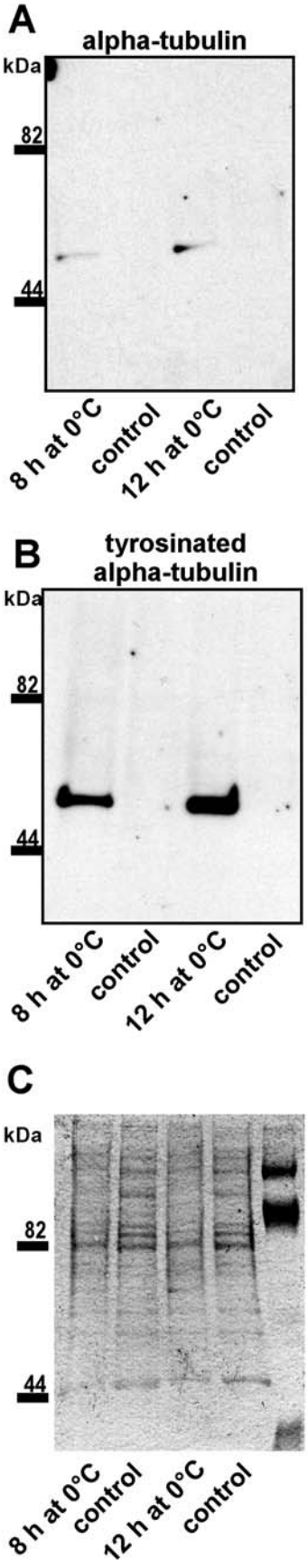

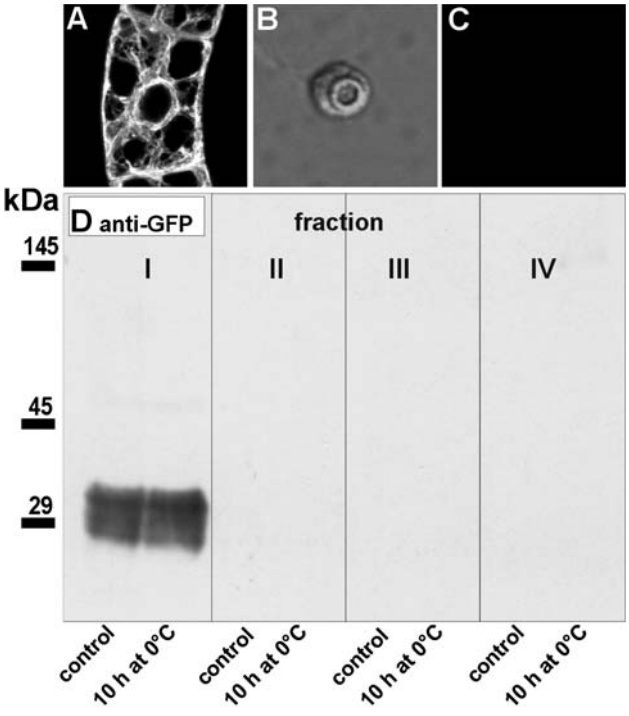

Fig. 5 A–D. Isolated nuclei are free from non-nuclear contamination. **A** The tobacco cell line BY-2-mGFP5-ER expressing mGFP5 fused at the N terminus to the signal peptide from *Arabidopsis thaliana* basic chitinase and at the C terminus to the endoplasmic-reticulum retention signal HDEL. A projection of eight optical sections (Z step size, 0.6 μm) through a central part of cell is shown. **B** and **C** DIC image (**B**) and GFP signal (**C**) of a nucleus isolated from a cell expressing mGFP5-ER maintained under control conditions. **D** Immunoblot detection of GFP protein in fractions collected during the isolation of nuclei. Fraction I, supernatant from the first centrifugation at 2000 **g**. Fraction II, nuclei before loading onto the Percoll gradient. Fraction III, supernatant from the last centrifugation at 2000 **g**. Fraction IV, sediment from the last centrifugation at 2000 **g** (purified nuclei). 10 μg of total protein were loaded per lane. Note that all GFP remained in fraction I

found in extracts from cold-treated nuclei was possibly caused by contamination with nonnuclear, but sedimentable, proteins. The transgenic cell line BY-2-mGFP5-ER used in this experiment constitutively expresses mGFP5 fused at the N terminus to the signal peptide from *Arabidopsis thaliana* basic chitinase and at the C terminus to the endoplasmic-reticulum retention signal (the HDEL peptide) (Petrášek et al. 2003). This so-called mGFP5-ER fusion protein has been previously shown to localize to the endoplasmic reticulum (Haseloff et al. 1997) (Fig. 5A) and thus it can serve as a marker for perinuclear mem-

Fig. 4 A–C. Detection of tubulin in protein extracts from isolated nuclei. **A** and **B** Immunoblots stained with antibodies directed against α-tubulin (**A**) and tyrosinated α-tubulin (**B**). **C** Amido black stain of proteins separated by SDS-PAGE and blotted in parallel under the same conditions. 15 μg of total protein were loaded per lane

brane structures. Nuclei were isolated from BY-2-mGFP5-ER cells that had been cultivated under standard conditions and were examined under the epifluorescence microscope. No GFP signal was found in these isolated nuclei (Fig. 5B, C). When different fractions from the isolation procedure were tested by Western blot analysis using an anti-GFP antibody, the GFP signal was clearly present in the first supernatant, but absent in fraction IV that contained the purified nuclei, irrespective of whether they had been isolated from control or from cold-treated cells (Fig. 5D). Nevertheless, nuclei isolated from cold-treated cells by the same protocol contained abundant tubulin (Fig. 4A, B).

Both tubulin molecules contain putative nuclear-export sequences

Tubulins lack at least the canonical nuclear-import signals (data not shown). We screened various sequences of plant α- and β-tubulins for nuclear-export sequences (NES). We identified two putative NES in the α-tubulins and three in the β-tubulins (Tables 1 and 2). Moreover, according to our preliminary studies, the potential NES motifs 2α and 1β through 3β are also well conserved between plant and animal tubulins, whereas the NES 1α seems to be plant-specific (data not shown).

Discussion

We observed that tubulin accumulated in interphase nuclei during the response to prolonged chilling that progressively eliminated cortical microtubules, and that this phenomenon was fully reversible when the temperature was restored to 25 °C. Intranuclear accumulation of tubulin during chilling and its exclusion during rewarming was shown by immunofluorescence in situ, as well as in vivo using transgenic cell lines expressing GFP–α-tubulin. Another transgenic cell line that expresses a GFP marker for endoplasmic reticulum and nuclear envelope (mGFP5-ER) was used for the detection of tubulin in isolated nuclei. Nuclear preparations that were void of cytoplasmic contamination (as evident from the complete removal of the GFP signal) nevertheless contained

Table 1. Putative nuclear-export sequences in plant α-tubulins[a]

Plant and α-tubulin	Accession nr.	Putative NES 1α	Putative NES 2α
Arabidopsis thaliana			
TUA1	NP_176654	LGSLLLERLSV 149–159	LRFDGAINV 242–250
TUA2	NP_175423	LGSLLLERLSV 149–159	LRFDGAINV 242–250
TUA3	NP_197478	LGSLLLERLSV 149–159	LRFDGALNV 242–250
TUA4	NP_171974	LGSLLLERLSV 149–159	LRFDGAINV 242–250
TUA5	NP_197479	LGSLLLERLSV 149–159	LRFDGALNV 242–250
TUA6	NP_849388	LGSLLLERLSV 149–159	LRFDGALNV 242–250
Nicotiana tabacum			
NtTUA	AB052822	LGSLLLERLSV 149–159	LRFDGALNV 242–250
NtTUA1	AJ421411	LGSLLLERLSV 149–159	LRFDGALNV 242–250
NtTUA2	AJ421412	LGSLLLERLSV 149–159	LRFDGALNV 242–250

[a] Consensus sequence Z-X(1–4)-J-X(2–3)-Z-X-Z, where Z stands for Leu, Ile, or Val; J stands for Met, or Phe; X stands for any

Table 2. Putative nuclear-export sequences in *Arabidopsis thaliana* β-tubulins[a]

β-Tubulin	Accession nr.	Putative NES 1β	Putative NES 2β	Putative NES 3β
TUB1	NP_177706	LQLERINV 43–50	ICFRTLKL 211–218	LNSDLRKLAV 247–256
TUB2	NP_568959	LQLERINV 42–49	ICFRTLKL 210–217	LNSDLRKLAV 247–256
TUB3	NP_568960	LQLERINV 42–49	ICFRTLKL 210–217	LNSDLRKLAV 247–256
TUB4	NP_199247	LQLERIDV 42–49	ICFRTLKL 210–217	LNSDLRKLAV 247–256
TUB5	NP_564101	LQLERINV 43–50	ICFRTLKL 211–218	LNSDLRKLAV 247–257
TUB6	NP_196786	LQLERVNV 42–49	ICFRTLKL 210–217	LNSDLRKLAV 247–256
TUB7	P29515	LQLERVNV 42–49	ICFRTLKL 210–217	LNSDLRKLAV 247–256
TUB8	NP_568437	LQLERVNV 42–49	ICFRTLKL 210–217	LNSDLRKLAV 247–256
TUB9	P29517	LQLERINV 42–49	ICFRTLKL 210–217	LNSDLRKLAV 247–256

[a] For consensus sequence, see footnote of Table 1

tubulin, but only when the nuclei had been prepared from cold-treated cells. No tubulin signal was detected in nuclear preparations from cells that had not been exposed to low temperature.

Hitherto, reports of intranuclear tubulin have been scarce. This indicates that the separation of interphase and mitotic microtubular functions is correlated to a strict compartmentalization of tubulin. Intranuclear tubulin has been reported for the mouse cell line SV3T3 (Menko and Tan 1980). More recently, nonassembled $\alpha\beta_{II}$-tubulin heterodimers have been detected in cultured rat kidney mesangial cells (Walss et al. 1999). The β_{II} isoform was present exclusively in nuclei and could be reversibly removed from the nuclei by vinblastine treatment (Walss-Bass et al. 2003). The authors suggested that nuclear tubulin constitutes a pool of dynamic tubulin that might assist the rapid cell proliferation characteristic of cancer cells. In plant cells, intranuclear microtubule-like structures have been documented in *Aesculus hippocastanum* L. by electron microscopy (Barnett 1991). However, the function of these intranuclear microtubules remained enigmatic. In our study, the tubulin was apparently not present in the form of microtubules, but as nonassembled tubulin heterodimers.

Although intranuclear tubulin seems to be a fairly exotic phenomenon in animal and plant cells, it is quite common in primitive eukaryotes with closed mitosis, where the division spindle develops within the karyoplasm surrounded by a nuclear envelope. This type of mitosis is frequently found in certain protists, fungi, and algae (for a review, see Heath 1980). There is a mounting body of evidence that tubulin is imported into the nucleus along with components of MTOCs just prior to the onset of mitosis (*Aspergillus nidulans* [Ovechkina et al. 2003], spindle-pole body of *Saccharomyces cerevisiae* [Pereira et al. 1998]). The precise timing of this nuclear import with respect to the cell cycle suggests that, in these organisms, the presence and absence in the nucleus of cytoskeletal components that participate in mitosis is carefully regulated and represents an important checkpoint within the cell cycle. In animal and plant cells, the disassembly of the nuclear envelope that results in an immediate and perfect exposure of chromatin to tubulin (open mitosis) has evolved during evolution as a more effective mechanism. However, even under conditions of open mitosis, some components of the spindle regulation machinery are imported into the nucleus prior to mitosis. For instance, γ-tubulin already appears in the nucleus of *Vicia faba* in the G_2 phase (Binarová et al. 2000). It is important to note that the antagonistic process – active exclusion of αβ-tubulin heterodimer from the nucleus – must occur at the transition from M to G_1, when the daughter nuclei become enclosed by a new nuclear membrane, not only in cells with closed mitosis, but also in those with open mitosis. Moreover, independently of the respective type of mitosis, all interphase cells must efficiently exclude αβ-tubulin from the nucleus or prevent its entry because it is not found in interphase nuclei. These facts suggest that, in spite of substantial differences between open and closed mitosis, some mechanisms, such as the import of cytoskeletal components regulating polymerization of microtubules at the beginning of mitosis and export of tubulin at the end, must be preserved in all organisms in order to ensure proper cell cycle progression.

It remains to be asked how tubulin is actually kept out of the interphase nucleus. We show in the present work that this mechanism is impaired during chilling at 0 °C. Transport between the cytoplasm and the nucleus is mediated by NPCs residing in the nuclear envelope. Transport of molecules through the nuclear pores can be either nonselective (i.e., passive) or selective (i.e., active, mediated by numerous protein transporters). Passive diffusion is limited by the exclusion size of the NPC, which is approximately 50 kDa (for a review, see Talcott and Moore 1999). Although molecules of up to 60 kDa are in principle allowed to passively diffuse across NPC, the diffusion rate is very low for molecules over 50 kDa (Rose et al. 2004). Therefore, it is unlikely that αβ-tubulin heterodimers (110 kDa) can pass the pores without specific interaction with the nuclear transport machinery. The massive increase in the pool of free tubulin dimers in the cytoplasm as a consequence of cold-induced elimination of assembled microtubules (Pokorná et al. 2004) might simply overload highly selective transport through the nuclear envelope such that tubulin "leaks" into the nucleus. However, an excess of free tubulin dimers generated by other means (oryzalin treatment, inhibiting the assembly of dimers into microtubules) does not produce such an entry of tubulin into the nucleus. This suggests that intranuclear tubulin is specific to the cold response. Since low temperature affects biological membranes (Kacperska 1999, Örvar et al. 2000), a possible explanation would be that cold-induced membrane injuries allow a slow leakage of tubulin into the karyoplasm. However, passive leakage of tubulin into the karyoplasm occurring as a consequence of membrane damage cannot explain its striking accumulation in the karyoplasm resulting in a clear concentration gradient in response to chilling. The accumulation of intranuclear tubulin coupled with a much lower concentra-

tion in the surrounding cytoplasm suggests that it binds to an unknown intranuclear lattice. The affinity to this lattice seems to be rather strong since tubulin remained attached even during the isolation of nuclei.

The entry of tubulin into the nucleus seems to be perfectly reversible when the cells are rewarmed, because it is not detectable in nuclei within minutes of recovery, as evident from immunofluorescence microscopy results and from live cells expressing GFP. Since this process is so rapid, it is unlikely that tubulin disappearance reflects degradation; the half-life of tubulin has been shown to be cell cycle dependent, varying between 1 and 15 h in *Physarum polycephalum* (Ducommun and Wright 1989). Even degradation of regulatory proteins (enzymes) usually takes much longer. A specific mechanism that excludes tubulin from the karyoplasm and is strongly (but reversibly) inhibited by low temperature must be involved in the recovery processes. Rapid and complete exclusion of tubulin during the first minutes of rewarming is unlikely to be caused by simple diffusion since the temperature dependency of diffusion is relatively low. Moreover, we observed that the intranuclear tubulin is rich in tyrosinated α-tubulin indicating that this has not been incorporated into stable microtubules and thus might represent a highly dynamic reservoir for the assembly of new microtubules (Wiesler et al. 2002).

The rapid recovery of tubulin exclusion from the nucleus demonstrates that the membranes of the nuclear envelope are not damaged or perturbed irreversibly. The target of chilling seems rather to be the NPCs and indicates that import and/or export of tubulin must be somehow regulated. Tubulin lacks at least the canonical NLS (Ovechkina et al. 2003 and unpubl. results). It is clear, however, that the standard pathways of protein import must be complemented by additional import mechanisms, since several proteins lacking an obvious NLS can enter the nucleus in both plant and animal cells (Evans et al. 2004). Interestingly, the intranuclear tubulin in cultured rat kidney mesangial cells reported by Walss et al. (1999) entered nuclei only if the cells underwent mitosis (Walss-Bass et al. 2001). The authors suggested that tubulin was trapped by nuclear factors at the end of mitosis rather than being actually transported through the nuclear envelope. However, we searched for putative NES in tubulin molecules and identified 5 in the α- and β-tubulins. Though the functionality of these nuclear-export signals must be confirmed experimentally, their existence is consistent with a model in which tubulin is exported through the nuclear pores by means of the conventional nuclear transport machinery, most of the components of which, such as importins, exportins, Ran, RanGAP and others (for a review, see Dasso 2002), have also been identified in higher plants (Smith and Raikhel 1999, Merkle and Nagy 1997, Pay et al. 2002).

We interpret the presence of tubulin in the nuclei of cold-treated cells in the following way. Tubulin is exclusively cytoplasmic during interphase, probably because its presence in the interphasic nucleus could induce serious disorders of cell-cycle regulation. We hypothesize that the integrity of the nuclear membrane during interphase, when nuclear pores control the transport of molecules, is the main mechanism that ensures the sequestration of tubulin to the cytoplasm during interphase. The interaction of tubulin with chromatin is crucial during mitosis. For closed mitosis, tubulin is imported into the nucleus by an unknown mechanism, whereas for open mitosis, no tubulin transport through the nuclear membrane is required since the nuclear envelope breaks down at the onset of mitosis. However, when daughter nuclei are formed at the end of mitosis, new nuclear envelopes have to be reestablished and the pool of tubulin molecules from the disintegrated spindle has to be removed from the karyoplasm. At this stage, tubulin is excluded from nuclei, possibly utilizing the NES export signals conserved in all tubulins. The integrity of the nuclear envelope and the active transport through the nuclear pores are impaired during cold treatment, resulting in intranuclear accumulation of tubulin. In our future work, we would like to verify the functionality of the different NES signatures in tubulin and to identify the corresponding binding partners of the nuclear transport machinery in both the cyto- and the karyoplasm.

Acknowledgments

We thank S. Hasezawa for a kind gift of the transgenic BY-2 cell line GT16. We thank Jan Marc for critical reading of the manuscript. We also thank Vlasta Sakařová for excellent technical assistance. This work was supported by grants from the Ministry of Education, Youth, and Sports of the Czech Republic nr. VZ113100003 and nr. LN00A081 (to Z.O.), by the Volkswagen Foundation Nachwuchsgruppenprogramm and the EC-FP5 grant nr. QLK5 CT-2000-00357 (to P.N.).

References

Barnett JR (1991) Microtubules in interphase nuclei of *Aesculus hippocastanum* L. Ann Bot 68: 159–165

Baskin TI, Cande WZ (1990) The structure and function of the mitotic spindle in flowering plants. Annu Rev Plant Physiol 41: 277–315

Binarová P, Cenklová V, Hause B, Kubátová E, Lysák M, Doležel J, Bogre L, Dráber P (2000) Nuclear gamma-tubulin during acentriolar plant mitosis. Plant Cell 12: 433–442

Cande WZ (1990) Centrosomes: composition and reproduction. Curr Opin Cell Biol 2: 301–305

Dasso M (2002) The Ran GTPase: theme and variations. Curr Biol 12: R502–R508

Ducommun B, Wright M (1989) Variation of tubulin half-life during the cell cycle in the synchronous plasmodia of *Physarum polycephalum*. Eur J Cell Biol 50: 48–55

Evans DE, Bryant JA, Hutchinson C (2004) The nuclear envelope: a comparative overview. In: Evans DE, Hutchinson CJ, Bryant JA (eds) The nuclear envelope. BIOS Scientific Publishers, Abingdon, pp 1–8

Haseloff J, Siemering KR, Prasher DC, Hodge S (1997) Removal of a cryptic intron and subcellular localization of green fluorescent protein are required to mark transgenic Arabidopsis plants brightly. Proc Natl Acad Sci USA 94: 2122–2127

Hasezawa S, Kumagai F (2002) Dynamic changes and the role of the cytoskeleton during the cell cycle in higher plant cells. Int Rev Cytol 214: 161–191

Heath IB (1980) Variant mitoses in lower eucaryotes – indicators of the evolution of mitosis. Int Rev Cytol 64: 1–80

Kacperska A (1999) Plant responses to low temperature: signalling pathways involved in plant acclimation. In: Margesin R, Schinner F (eds) Cold-adapted organisms. Springer, Berlin, pp 79–104

Kumagai F, Yoneda A, Tomida T, Sano T, Nagata T, Hasezawa S (2001) Fate of nascent microtubules organized at the M/G(1) interface, as visualized by synchronized tobacco BY-2 cells stably expressing GFP-tubulin: time-sequence observations of the reorganization of cortical microtubules in living plant cells. Plant Cell Physiol 42: 723–732

Menko AS, Tan KB (1980) Nuclear tubulin of tissue culture cells. Biochim Biophys Acta 629: 359–370

Merkle T, Nagy F (1997) Nuclear import of proteins: putative import factors and development of in vitro import systems in higher plants. Trends Plant Sci 2: 458–464

Mirski SEL, Bielawski JC, Cole SPC (2003) Identification of functional nuclear export sequences in human topoisomerase II alpha and beta. Biochem Biophys Res Commun 306: 905–911

Mizuno K (1992) Induction of cold stability of microtubules in cultured tobacco cells. Plant Physiol 100: 740–748

Nagata T, Nemoto Y, Hasezawa S (1992) Tobacco BY-2 cell line as the "HeLa" cell in the cell biology of higher plants. Int Rev Cytol 132: 1–30

Örvar BL, Sangwan V, Omann F, Dhindsa RS (2000) Early steps in cold sensing by plant cells: the role of actin cytoskeleton and membrane fluidity. Plant J 23: 785–794

Ovechkina Y, Maddox P, Oakley CE, Xiang X, Osmani SA, Salmon ED, Oakley BR (2003) Spindle formation in Aspergillus is coupled to tubulin movement into the nucleus. Mol Biol Cell 14: 2192–2200

Pay A, Resch K, Frohnmeyer H, Fejes E, Nagy F, Nick P (2002) Plant RanGAPs are localized at the nuclear envelope in interphase and associated with microtubules in mitotic cells. Plant J 30: 699–709

Pereira G, Schiebel E (1997) Centrosome-microtubule nucleation. J Cell Sci 110: 295–300

Pereira G, Knop M, Schiebel E (1998) Spc98p directs the yeast gamma-tubulin complex into the nucleus and is subject to cell cycle-dependent phosphorylation on the nuclear side of the spindle pole body. Mol Biol Cell 9: 775–793

Petrášek J, Černá A, Schwarzerová K, Elčkner M, Morris DA, Zažímalová E (2003) Do phytotropins inhibit auxin efflux by impairing vesicle traffic? Plant Physiol 131: 254–263

Pokorná J, Schwarzerová K, Zelenková S, Petrášek J, Janotová I, Čapková V, Opatrný Z (2004) Sites of actin filament initiation and reorganization in cold-treated tobacco cells. Plant Cell Environ 27: 641–653

Popov N, Schmitt S, Mathies H (1975) Eine störungsfreie Mikromethode zur Bestimmung des Proteingehaltes in Gewebshomogenaten. Acta Biol Germ 34: 144–146

Rose A, Patel S, Meier I (2004) Plant nuclear envelope proteins. In: Evans DE, Hutchinson CJ, Bryant JA (eds) The nuclear envelope. BIOS Scientific Publishers, Abingdon, pp 69–88

Shimamura M, Brown RC, Lemmon BE, Akashi T, Mizuno K, Nishihara N, Tomizawa KI, Yoshimoto K, Deguchi H, Hosoya H, Mineyuki Y (2004) Gamma-tubulin in basal land plants: characterization, localization, and implication in the evolution of acentriolar microtubule organizing centers. Plant Cell 16: 45–59

Smith HMS, Raikhel NV (1999) Protein targeting to the nuclear pore. What can we learn from plants? Plant Physiol 119: 1157–1163

Stoppin-Mellet V, Peter C, Lambert AM (2000) Distribution of gamma-tubulin in higher plant cells: cytosolic gamma-tubulin is part of high molecular weight complexes. Plant Biol 2: 290–296

Talcott B, Moore MS (1999) Getting across the nuclear pore complex. Trends Cell Biol 9: 312–318

Walss C, Kreisberg JI, Luduena RF (1999) Presence of the beta(II) isotype of tubulin in the nuclei of cultured mesangial cells from rat kidney. Cell Motil Cytoskeleton 42: 274–284

Walss-Bass C, Kreisberg JI, Luduena RF (2001) Mechanism of localization of beta(II)-tubulin in the nuclei of cultured rat kidney mesangial cells. Cell Motil Cytoskeleton 49: 208–217

Walss-Bass C, Kreisberg JI, Luduena RF (2003) Effect of the antitumor drug vinblastine on nuclear beta(II)-tubulin in cultured rat kidney mesangial cells. Invest New Drug 21: 15–20

Wick SM, Seagull RW, Osborn M, Weber K, Gunning BES (1981) Immunofluorescence microscopy of organized microtubule arrays in structurally stabilized meristematic plant cells. J Cell Biol 89: 685–690

Wiese C, Zheng YX (1999) Gamma-tubulin complexes and their interaction with microtubule-organizing centers. Curr Opin Struct Biol 9: 250–259

Wiesler B, Wang QY, Nick P (2002) The stability of cortical microtubules depends on their orientation. Plant J 32: 1023–1032